Biophysical Chemistry 23 (1985) 115–124
Elsevier

BPC 01030

AGGREGATION OF BOVINE SERUM ALBUMIN UPON CLEAVAGE OF ITS DISULFIDE BONDS, STUDIED BY THE TIME-RESOLVED SMALL-ANGLE X-RAY SCATTERING TECHNIQUE WITH SYNCHROTRON RADIATION

Tatzuo UEKI [a], Yuzuru HIRAGI [b], Mikio KATAOKA [c], Yōji INOKO [a], Yoshiyuki AMEMIYA [d], Yoshinobu IZUMI [e], Hiroyuki TAGAWA [f] and Yoshio MUROGA [g]

[a] *Department of Biophysical Engineering, Faculty of Engineering Science, Osaka University, Toyonaka, Osaka 560,* [b] *Institute for Chemical Research, Kyoto University, Uji, Kyoto 611,* [c] *Faculty of Science, Tohoku University, Sendai, Miyagi 980,* [d] *Photon Factory Instrumentation Group, National Laboratory for High Energy Physics, Oho-Machi, Tsukuba-Gun, Ibaraki 305,* [e] *Faculty of Science, Hokkaido University, Sapporo, Hokkaido 060,* [f] *Faculty of Science and Technology, Nihon University, Chiyoda-Ku, Tokyo 100, and* [g] *Faculty of Engineering, Nagoya University, Nagoya, Aichi 464, Japan*

Received 16th January 1985
Revised manuscript received 18th June 1985
Accepted 5th September 1985

Key words: Bovine serum albumin; SAXS; Synchrotron radiation; Aggregation; Dithiothreitol

A rapid mixing system of the stopped-flow type, used with small-angle X-ray scattering equipment using synchrotron radiation, is described. The process of aggregation of bovine serum albumin was traced with a time interval of 50 s, initiated upon cleavage of its disulfide bonds by reduction with dithiothreitol. The results indicate that a 218-fold molar excess of dithiothreitol over the number of moles of disulfide bonds in bovine serum albumin is sufficient to initiate the reaction immediately after mixing, which reaches equilibrium in about 15 min. On the other hand, half this amount is not sufficient to initiate the reaction, so that the reaction is delayed by about 150 s. Such a single-shot time-resolved experiment showed that experiments with a time interval of 100 ms are possible with repeated multi-shot runs.

1. Introduction

Synchrotron radiation, emitted from a storage ring, is a powerful source of X-rays for small-angle scattering because of its prominent features of high intensity, wavelength continuum and low divergence. In particular, its high intensity has opened up the possibility of time-dependent scattering measurement from solutions to investigate the kinetics of biologically important transient phenomena [1,2]. This method can be applied to studies of enzymatic reactions, assembly/disassembly of biological systems, denaturation/renaturation and phase transitions, studied so far spectroscopically by techniques such as stopped-flow rapid mixing, temperature jump and flash photolysis. The advantage of small-angle X-ray scattering (SAXS) over spectroscopic methods may be that the SAXS reflects directly the structure of a molecule (or particle) itself.

To realize time-dependent measurements of SAXS, optics that is optimized for the flux of synchrotron radiation [3–6], a position-sensitive detector of high performance [7] and fast data acquisition systems have recently been developed in some synchrotron radiation facilities.

We have designed a small-angle scattering equipment (SAXES) for the use of synchrotron radiation [8], set up at the Photon Factory in the National Laboratory for High Energy Physics, Tsukuba. A specimen chamber for stopped-flow mixing and the associated data acquisition system have also been developed. The present paper describes the performance of the time-resolved ex-

periment system, with the use of the aggregation process of bovine serum albumin (BSA) molecules. The aggregation reaction of BSA was initiated upon cleavage of its disulfide bonds by dithiothreitol (DTT) reduction. BSA and DTT solutions were rapidly mixed in a stopped-flow mixing chamber and the subsequent reaction was monitored by means of the small-angle scattering from the mixture. Preliminary results, analysed from the Guinier plots [9,10], will be described.

2. Materials and methods

2.1. Reaction

BSA of globulin-free grade was purchased from Sigma Chemical Co. (lot 33F-9325) and used without further purification. The following reaction conditions were adopted to ensure a reasonable reaction rate for evaluation of the present stopped-flow apparatus, from preliminary light scattering experiments (Nakatani, personal communication). BSA was dissolved in 50 mM phosphate buffer containing 0.15 M NaCl, pH 8.0. Reaction was performed with BSA concentrations of either 0.5% (w/v) (0.07 mM) or 1.0% (w/v) (0.15 mM). The pH values of solutions were measured to be 7.90 and 7.85 for 0.5% and 1.0% BSA solutions, respectively, deviating slightly from the pH of the buffer solution because of weak buffering capacity. The reaction mixture contained 280 mM DTT. This concentration corresponds to about 218- and 110-fold molar excess over the number of moles of disulfide bonds in 0.5 and 1.0% BSA, respectively, since each BSA molecule contains 17 disulfide bonds [11]. The aggregation of BSA molecules is initiated by unfolding of the peptide chains upon cleavage of their disulfide bonds by reduction with DTT. The temperature of reaction was 25–27°C.

2.2. Stopped-flow specimen chamber

The BSA-DTT reaction was performed by rapid mixing with a stopped-flow apparatus. The apparatus was manufactured by Unisoku, modified from the original design of Nagamura et al. [12]. It adopted the double-syringe type as shown in fig. 1. A single shot of mixing requires equal volumes of solutions, 500 μl in total, though a total of 250 μl per shot is also possible. The specimen chamber has a cross-section of 4 width × 6 height mm^2 with an X-ray path length of 1 mm. The initial perturbation after mixing, i.e., cavitation in mixed solution and oscillation of X-ray path length, is suppressed within 20 ms (Kihara and Nagamura, personal communication).

2.3. Small-angle X-ray scattering optics and detector

The SAXS experiments were carried out on a focusing optics, SAXES, installed at the 2.5 GeV storage ring in the Photon Factory of the National

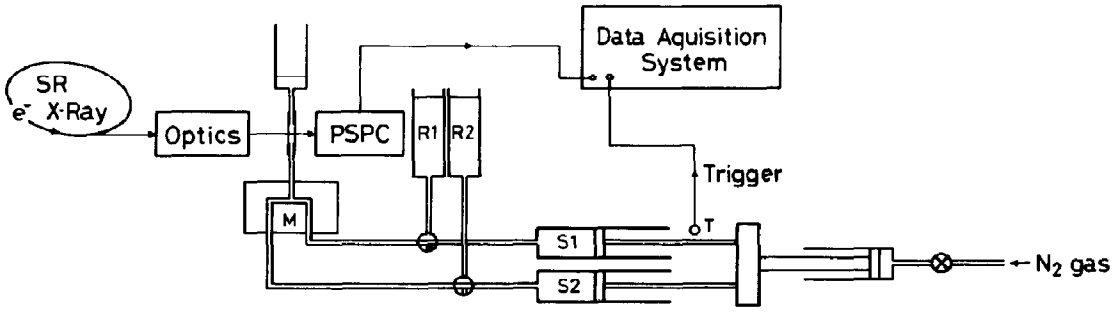

Fig. 1. Outline of the stopped-flow rapid mixing apparatus used with SAXES in the Photon Factory, National Laboratory for High Energy Physics, Tsukuba. R1 and R2, reservoirs of reactant solutions; S1 and S2, pair of syringes; M, mixing chamber. The chamber between the optics and PSPC (position-sensitive proportional counter) is the specimen chamber. A trigger pulse immediately after mixing initiates the data acquisition system. Actions of valves and syringes are controlled by pressure of N_2 gas.

Laboratory for High Energy Physics at Tsukuba. SAXES employs a novel optics of double flat-crystal monochromators followed by a bent cylindrical mirror, yielding a point focus in the rear focal plane with 1 : 1 magnification [8]. Unlike the toroidal mirror-type optics, SAXES has a small-angle resolution of Bragg spacing 1000 Å or better, realized by placing the 'guard' slit further from the mirror in front of the specimen. The optics also has the advantage of easy tunability of wavelength. In the present work, the wavelength used was 1.54 Å and the specimen-to-detector distance was about 1900 mm. The circulating current of electrons in the storage ring was 70–150 mA. Details of the optics and its performance can be referred to elsewhere [8].

The SAXS intensity was recorded with a one-dimensional position-sensitive proportional counter and associated electronic circuits [8]. The counter probe was flushed with a 90% argon + 10% CH_4 mixture at a gauge pressure of 1 atm. The positions of X-rays in the probe, whose effective length is 200 mm, are determined with a fast delay line of 400 ns.

2.4. Data acquisition system

The effective length of the counter probe is divided into 512 channels, which correspond to the scattering angles. The data acquisition scheme is shown in fig. 2. For each stopped-flow shot, 30 spectra were recorded at intervals of 25 or 50 s. In

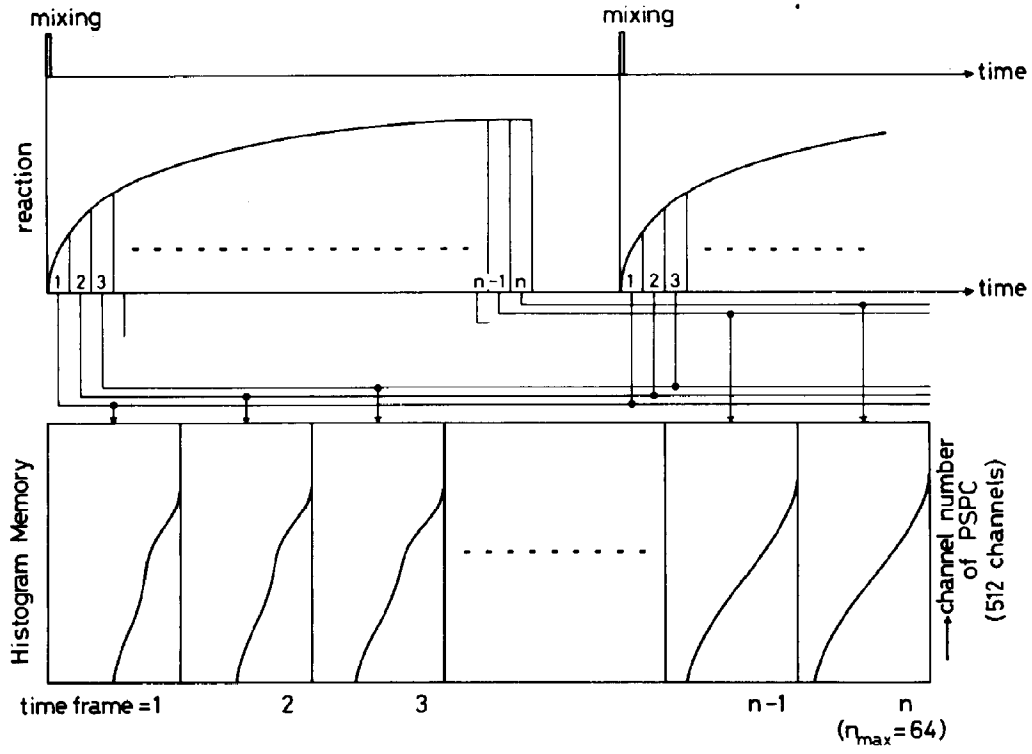

Fig. 2. The data acquisition scheme in SAXES. The small-angle scattering profiles of each time frame are recorded in 512 channels of histogram memories which carry a total of 32 K words with a depth of 24 bits, in accordance with the reaction time. Thus, a total of 64 time frames can be recorded in a single experiment. The minimum interval of reaction time recorded is less than 1 ms.

the present paper, we describe the results of a single-shot mixing experiment to show the performance of the system, though accumulation of shots certainly improves the quality of the scattering data.

All scattering data were corrected for variation in intensity of the primary beam which is monitored by an ionization chamber placed in front of the specimen. Since the optics of SAXES is of the 'point' focusing type, the intensity data were used without slit correction for further data treatments. The data treatments were carried out on a PDP 11/34 minicomputer (Digital Equipment Corp.).

2.5. Interpretation of small-angle scattering data

The SAXS intensity from a dilute solution of particles, $I(S)$, is proportional to the number of particles, n, the square of the scattering mass which is equal to the volume V multiplied by the excess electron density, $\Delta\rho$, and a characteristic shape function, $i(S)$ [9,13]:

$$I(S) \propto n(V\Delta\rho)^2 i(S) \tag{1}$$

where S is the reciprocal coordinate, $2 \sin\theta/\lambda$ (2θ, scattering angle, λ, wavelength of X-rays).

The structural parameters, which are directly obtained from $I(S)$ or $i(S)$, are the radius of gyration of particle, R_g, and the degree of aggregation. The radius of gyration is calculated from the slope of a straight line of a Guinier plot, a plot of logarithm of intensity vs. S^2 [9.10].

$$\frac{\mathrm{d}[\ln I(S)]}{\mathrm{d}[S^2]} = -(1/3)(2\pi S)^2 R_g^2 \tag{2}$$

in which S is limited in the small-angle region. R_g increases, of course, as the particles aggregate as well as the particle expands. When the solution is composed of several types of particles, i.e., not monodisperse, the total curve is still represented by an exponential function if the Guinier approximation is valid for all individual particles [9]. The radius of gyration of the system is the weighted average:

$$R^2_{g\ \mathrm{average}} = \frac{\sum_k p_k n_k^2 R^2_{g\,k}}{\sum_k p_k n_k^2} \tag{3}$$

where p_k, n_k and $R_{g\,k}$ are the molar fraction, number and radius of gyration of the k-th type of particle.

The intensity, $I(0)$, as obtained from the extrapolation of $I(S)$ to $S = 0$, is given as

$$I(0) \propto n(V\Delta\rho)^2 \tag{4}$$

as $i(0) = 1$. Provided that all particles in the solution aggregate in dimeric form, the number of particles is halved whereas $(V\Delta\rho)^2$ increases 4-fold since the volume becomes twice as large. As a result, $I(0)$ of a dimer solution increases twice as much compared with that of a monomer solution. Hence, the degree of aggregation can be dictated by $I(0)$.

The 'total' intensity, which was referred in some papers [14,15], is defined as

$$\text{total intensity} = \int_0^{S_{\max}} I(S)\mathrm{d}S \tag{5}$$

This is different from the 'integrated' intensity $\int_0^\infty I(S)S^2\mathrm{d}S$. Since the integrated intensity is invariant as is well-known from Parseval's theorem [16], it remains unchanged even when the system changes in any way. The total intensity seems to be the qualitative measure of $I(0)$, since the range of integration stays within some small-angle region, $S_{\max}$.

3. Results and discussion

3.1. Small-angle scattering from BSA solution

A static measurement of SAXS from 0.5% (w/v) BSA in 50 mM phosphate buffer containing 0.15 M NaCl, pH 8.0, was carried out prior to the stopped-flow mixing experiments. The counting time was 300 s for BSA solution and background (buffer) with the receiving slit height of 2 mm in front of the position-sensitive counter probe. The slope of the Guinier plot (fig. 3), in the range $10–150 \times 10^{-6}$ Å^{-2} in S^2 (corresponding Bragg spacing of about 300–80 Å), gave the radius of gyration of the particle as 28.5 ± 0.4 Å calculated by the least-squares method. This value is comparable to that (29.8 Å) under isoionic conditions of pH 5.3 [18]. In these conditions, the BSA mole-

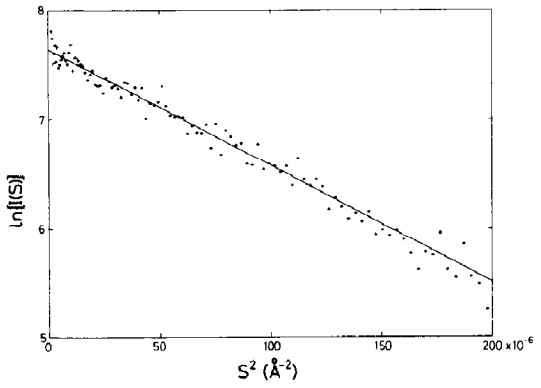

Fig. 3. Guinier plot, $\ln[I(S)]$ vs. S^2, of the scattering profile from a 0.5% BSA solution in 50 mM phosphate buffer, pH 8.0, containing 0.15 M NaCl. The $\ln[I(S)]$ is the natural logarithm of the small-angle scattering profile where S is the reciprocal parameter equal to $2 \sin \theta/\lambda$ ($Å^{-1}$). The innermost data point corresponds to the Bragg spacing of about 1,000 Å (see also the abscissa of fig. 4). The straight line gives the slope of data points from the least-squares method, giving a radius of gyration of 28.6 ± 0.4 Å. A static measurement was made with a counting time of 300 s. The plots depict the results obtained after correcting for background scattering from buffer solution of the same counting time.

cules are considered to be compact and monomeric in solutions. At pH values below about 4, a BSA molecule undergoes a striking, reversible structural transition [19]. Small-angle studies on BSA at pH 3.6 resulted in a radius of gyration of 68.5 Å (F-form) [18] instead of 30.6 Å (N-form): part of the peptide chain unravels to become a loose random coil-like structure (estimated to be about 35%), the rest of the molecule folded remaining in a compact form. More detailed analysis also revealed that the solution at pH 3.6 contained about 20% by weight of dimeric BSA [20].

A sedimentation velocity study of a BSA solution under isoelectric conditions of pH 4.65 showed no evidence of any peaks other than the main one [17]. However, a slight asymmetry of the main peak indicated a small proportion of BSA dimers [17]: such a small amount of dimer component should not have a significant effect on the scattering curves. The reduction of disulfide bonds in BSA by DTT has an equilibrium constant of about 10^4 at pH 7 [21], and the reduction is usually conducted under basic pH conditions [22,23]. No SAXS studies on BSA at basic pH have been carried out, in contrast to the experiments at acidic pH. Since we have not performed a sedimentation velocity study, we have no evidence that the BSA molecule is a monomer at pH 8.0 in 50 mM phosphate buffer, pH 8.0, containing 0.15 M NaCl. From comparison of the radii of gyration and the fact that even 5% contamination by dimers results in an increase of the radius of gyration of only about 2% [17], we assumed that the BSA molecules are mostly monomers in a compact form at pH 8.0, together with the reason that the change in radius of gyration in the present study deals with a much larger change on values. Thus, the radius of gyration, 28.6 Å, was taken as the initial value in BSA-DTT reaction.

3.2. Time-resolved measurements of small-angle scattering from BSA-DTT reaction mixture

The SAXS intensities were recorded in each time frame immediately after mixing of the BSA and DTT solutions by stopped-flow mixing apparatus, with intervals of either 25 or 50 s. In the following, the data with time intervals of 50 s will by referred to, since the reaction reaches the final stage after more than 10 min, as shown later. The concentration of BSA in the reaction mixture was either 0.5% (w/v) or 1.0% (w/v), i.e., either 1% or 2% BSA solution was mixed with an equal volume of buffer solution containing DTT.

The raw SAXS profiles are shown in fig. 4: time frames 1, 4, 8 and 12 were plotted for a 0.5% BSA solution, the background scattering being depicted as a dotted line. It can be seen that the first frame has an appreciable intensity above the background scattering at rather higher scattering angles whereas the others evidently display a marked increase in intensity at smaller scattering angles. The SAXS intensities, $I(S)$ values, were obtained from the raw scattering profiles by correcting the background scattering from buffer containing 50 mM phosphate, 0.15 M NaCl and DTT.

The total intensities were plotted for each time frame of the reaction of 0.5 and 1% BSA in fig. 5. Since scaling of the curves was not carried out with respect to the concentration of BSA and variation of primary beam intensity of X-rays, the

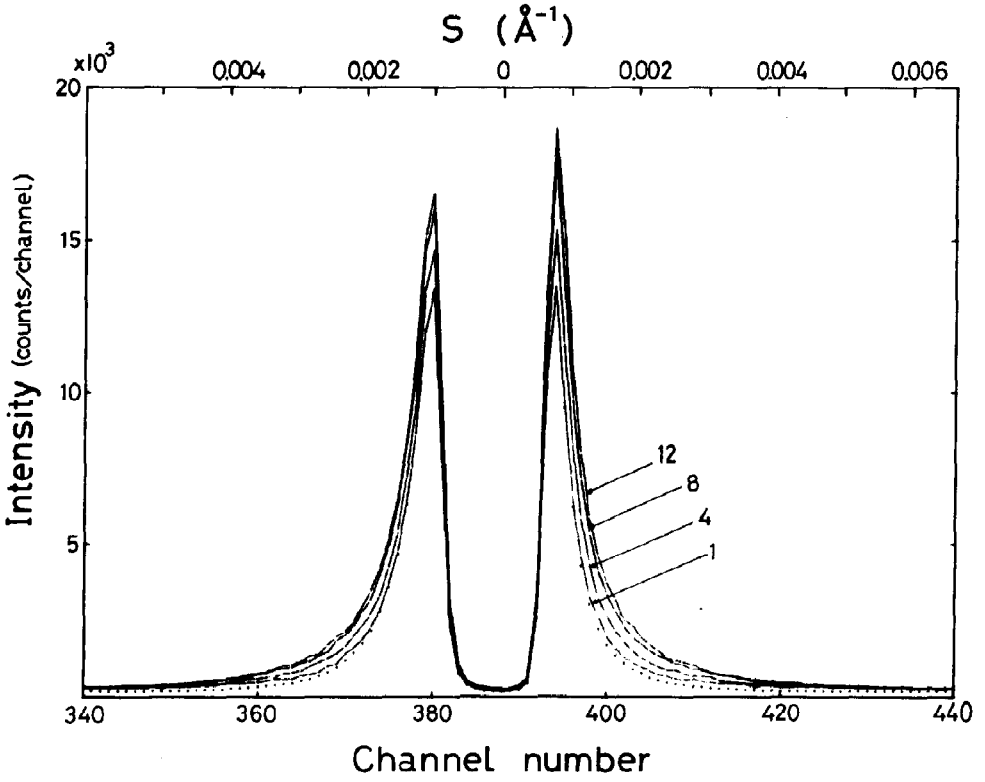

Fig. 4. Raw small-angle scattering profiles of time-resolved measurement of BSA-DTT reaction. Time frames 1, 4, 8 and 12 are plotted as solid lines and the background scattering as the dotted line. Each time frame is the result of 50 s counting time. Note the remarkable increase in intensities in the small-angle region of time frames 4, 8 and 12.

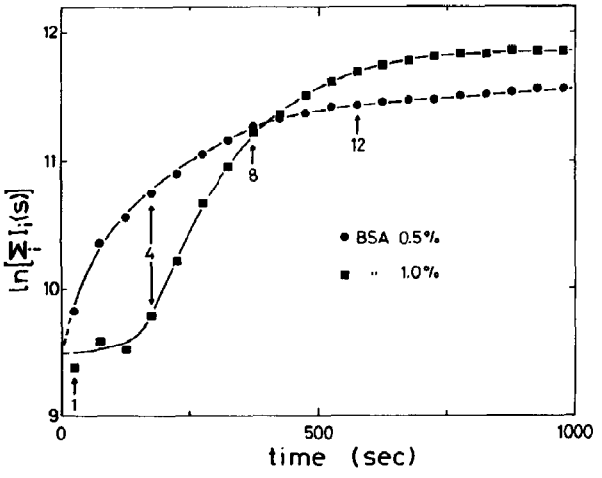

Fig. 5. Plots of total intensities of each small-angle scattering profile obtained from the BSA-DTT reaction mixture, with a time interval of 50 s. (●) 0.5% BSA, (■) 1.0% BSA. Numbers 1, 4, 8 and 12, are the time frames corresponding to those in fig. 4. Note that the changes in total intensities reach equilibrium after about 15 min from the initiation of reaction.

values on the ordinate are relative. As expected from fig. 4, the total intensities increase appreciably for the plot for 0.5% BSA and approach the final stage of reaction in about 10 min (time frame 12). An interesting observation from the plots in fig. 5 is the time delay of about 150 s in the initial rise of the reaction of 1% BSA. Accordingly, the final stage occurs in about 750 s. The accessibility of disulfide bonds to reduction by DTT is reported to show a strong pH dependence around pH 7–8 [24]. The pH values measured were 7.90

and 7.85 for 0.5 and 1.0% BSA solutions, respectively. The accessibility is greater at higher pH [24] and the reaction may be expected to proceed faster for a 0.5% solution although the difference in pH values for both solutions seems to be minimal. Thus, this delay is probably due to the molar ratio [DTT]/[BSA] in both solutions. As stated in section 2.5, the meaning of total intensity is unclear and limited, so that the following discussion will thereafter focus on the radius of gyration and the intensity at $S = 0$, $I(0)$.

3.3. Treatment of time-resolved data of small-angle scattering profiles

The Guinier plots, $\ln[I(S)]$ vs. S^2, of time-resolved measurement of scattering from a 0.5% BSA reaction mixture are shown in fig. 6 for time frames 1, 4, 8 and 12. The plots are displaced vertically by an arbitrary amount for clarity. The plot of the first frame is very similar to that of the static measurement shown in fig. 3. A typical Guinier plot of scattering from a reaction mixture, e.g., that of the fourth time frame, seems to be represented by at least three straight lines in the respective small-angle regions, I, II and III (see inset to fig. 6): component I has a radius of gyration $R_g = 142$ Å corresponding to the line approximated in $1\text{–}5 \times 10^{-6}$ Å^{-2}, component II has $R_g = 49$ Å in $20\text{–}50 \times 10^{-6}$ Å^{-2} and component III has $R_g = 30$ Å in $50\text{–}150 \times 10^{-6}$ Å^{-2}. The steep increase seen in frames 4, 8 and 12 in the very small-angle region I corresponds to an early change of the system in the BSA-DTT reaction mixture, and not to artifacts arising from the apparatus. These increases are observed 25 s after the reaction starts and reach equilibrium with 100 s. Since, as compared with the time course of disulfide bond reduction studied biochemically, this change seems to proceed too fast, it is considered to occur from a small amount of impurity, possibly the A-form of BSA [25], reacting with DTT. Therefore, we will not pursue this point.

Component III, which gives a straight line in the region $50\text{–}150 \times 10^{-6}$ Å^{-2} in the Guinier plot, is the other component of particles in solution which is difficult to interpret. As seen in fig. 6, the data points in this region scatter very widely except for that of the first frame. Because the counts per channel in those frames other than the first are not appreciably low compared with those of the first, the scatter of data points must by attributed to a property of component III. It is possible to calculate the radius of gyration in this region by the least-squares method, which converges to about 44 Å in 15 min. However, we shall not discuss component III further, since the errors in the data and radius of gyration are too large to interpret.

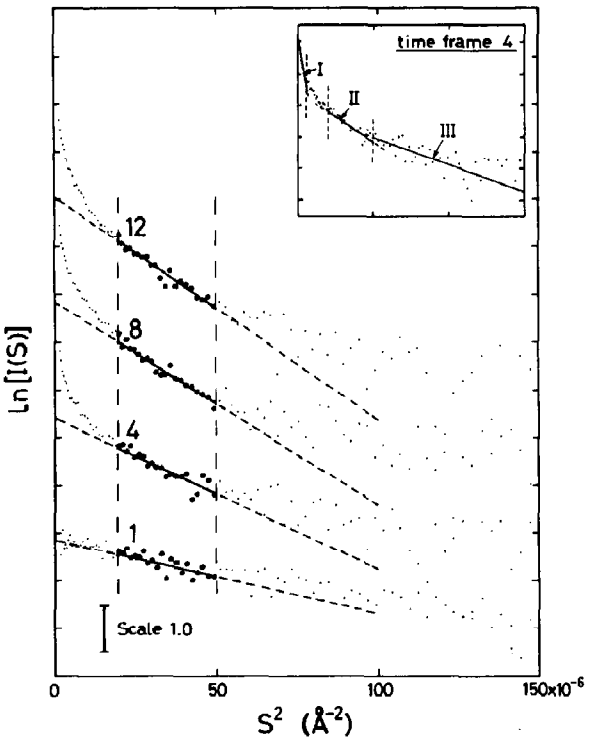

Fig. 6. Guinier plots of small-angle scattering profiles of time-resolved measurements on BSA-DTT reaction mixture. Time frames 1, 4, 8 and 12 are plotted. The plots are from the original raw data shown in fig. 4. The ordinates are shifted vertically by an arbitrary amount for clarity. The straight lines are the results of least-squares fitting in region II of $20\text{–}50 \times 10^{-6}$ Å^{-2} of component II (data points in the region denoted by filled circles). (Inset) Small-angle regions of I, II and III for data points from time frame 4.

3.4. Aggregation behavior of BSA molecules

Component II in the reaction mixture corresponds to particles resulting in a straight line in

the region $20-50 \times 10^{-6}$ Å^{-2} in the Guinier plots (see inset to fig. 6.). The time course of the change in the radius of gyration is plotted in figs. 7 and 8 for 0.5 and 1% BSA solutions respectively: the initial stage has an R_g value of 29 Å, the final equilibrium having an R_g value of about 60 Å. As quoted in section 3.3, the BSA molecule undergoes a transition below pH 4 [19] and was demonstrated to have an unfolded segment in addition to the compact form at pH 3.6, giving a radius of gyration of about 69 Å [18]. Although the solution contains 20% by weight of BSA dimers and the radius of gyration is affected by the dimer to some extent, the increase in the radius of gyration as an unfolded monomer is remarkable. Thus, the question is whether the increase in radius of gyration of particles in the BSA-DTT reaction mixture is attributable to the unfolded segment of the

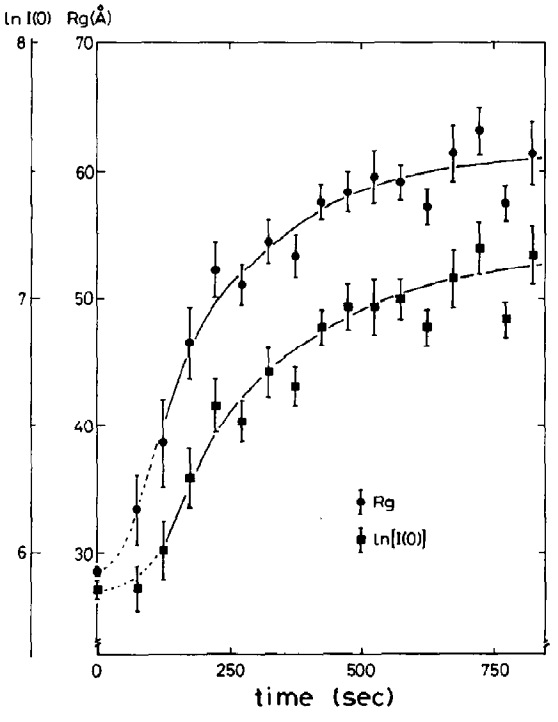

Fig. 7. Plots of radius of gyration and $\ln[I(0)]$ for 0.5% BSA solution, obtained from the Guinier plots, of which typical traces are shown in fig. 6. The time delays in the initial rise are unclear, but the errors in these data points make its meaning less significant.

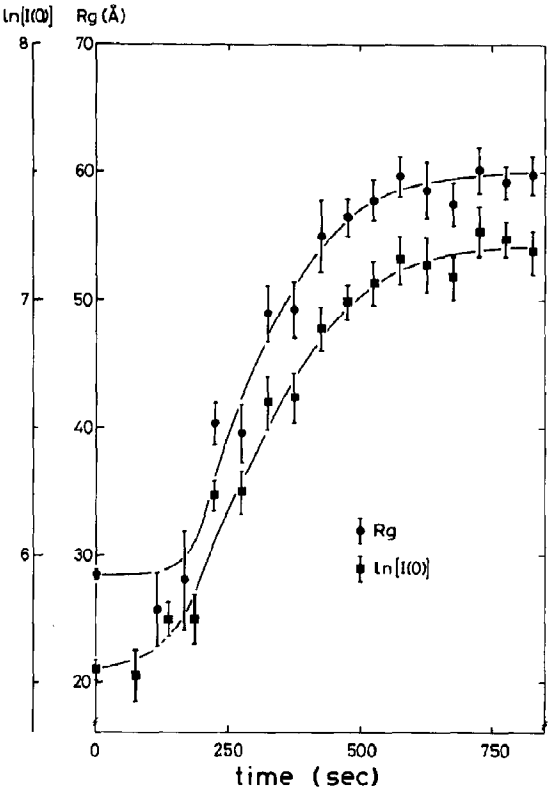

Fig. 8. Plots of radius of gyration and $\ln[I(0)]$ for 1.0% BSA solution, obtained from the Guinier plots of time-resolved measurement of small-angle scattering profiles. The time delay in the initial rise is very obvious in these plots.

monomeric molecule. The experiment at pH 3.6 on an absolute scale indicated that the molecular weight of the particles, as determined by the small-angle experiment, does not change, resulting in an essentially constant $I(0)$ value [18].

The present time-resolved measurements, though not on an absolute scale, clearly show a marked increase in the $I(0)$ values as seen in figs. 7 and 8: about 4-times as large in the 15th time frame as the initial value for the 0.5% BSA reaction and about 5-times as large for 1% BSA. These data, as understood from eq. 4, evidently demonstrate the aggregation of partially reduced or reduced BSA monomers, probably as a result of unfolding of the compact form by cleavage of disulfide bonds in the monomers. This reaction

can be represented by a number of equilibria as follows:

$$A \rightleftharpoons A'$$
$$A'_k + lA' \rightleftharpoons A'_{k+l} \quad (k, l = 1, 2 \ldots) \qquad (6)$$

where A is monomeric BSA in the native state and A′ the monomer with a partially unfolded structure. The second equation denotes a number of reactions: this equation indicates that a k-meric A′ particle reacts with l moles of A′ to result in a $(k + l)$-meric A′ particle, for example. Certainly, k-meric and l-meric particles react to produce $(k + l)$-meric A′ particles. We do not have parameters such as the equilibrium constants of such reactions in the final stage of the reaction mixture available, except for the behavior of the $I(0)$ values. Therefore, the numbers of monomers involved in aggregation are estimated to be at least four in the particles of the 0.5% BSA-DTT reaction mixture and five for the 1% BSA-DTT mixture, assuming that the equilibrium is completely to the right and that the degree of hydration does not change upon aggregation of monomers.

As seen in fig. 5, a delay in the reaction is evident between the data for 0.5 and 1% BSA from figs. 7 and 8. The delay in the initial increase in the radius of gyration and $\ln[I(0)]$ for 0.5% BSA, as seen in fig. 7, is unclear due to large errors. On the other hand, the delay is evident for the 1% BSA reaction mixture, the delay being about 150 s, consistent with that of the total intensity in fig. 5. As discussed in section 3.3, this delay is not attributable to the pH difference in 0.5 and 1.0% BSA solutions, but to the molar ratio of [DTT]/[BSA] in both solutions. The disulfide bonds in proteins are classified into three groups with respect to their relative reactivity [22]: fully exposed (reactive with 0.5 mM dithioerythritol), partly buried (reactive with 10 mM dithioerythritol) and buried (unreactive in the native state without denaturing reagents). For complete reduction, a 50-fold molar excess of DTT over the number of moles of disulfide bonds in the protein molecule is necessary, in addition to a denaturing reagent such as urea or guanidine hydrochloride to unfold the polypeptide chain and expose all the disulfide bonds [21]. Even for limited reduction, an about 60-fold molar excess of DTT is required over the number of moles of γ_G-immunoglobulin [26], and this amount is dependent on the nature of proteins. In the present reaction mixture, a 218- and 110-fold molar excess of DTT was added with respect to the number of moles of disulfide bonds in 0.5 and 1.0% BSA without any denaturing reagent. Such an amount of DTT seems to be about the critical concentration, resulting in a definite time being necessary in the first reaction of eq. 6 and a delay time occurs in the 1.0% BSA solution as compared with that of the 0.5% BSA solution. Therefore, the SAXS results obtained from 0.5 and 1% BSA-DTT reaction mixtures differ from each other on account of the delay time of the reaction, leaving the rest of the time course of the reaction approximately parallel.

A 218-fold molar excess of DTT is certainly sufficient to unfold the polypeptide chain of 0.5% BSA by reducing fully exposed or partly buried disulfide bonds without appreciable reaction time, and aggregation initiates immediately after mixing of the solutions. On the other hand, a 110-fold molar excess of DTT in the 1% BSA solution is probably insufficient to reduce the minimum number of disulfide bonds to unfold the polypeptide chain to cause aggregation. About 150 s after mixing, DTT reduces a sufficient number of disulfide bonds to induce aggregation of BSA monomers. After the initial rise of the reaction, the concentration of BSA (1%) accelerates the aggregation reaction so that aggregation tends to proceed a little faster than that of the 0.5% BSA reaction mixture.

3.5. Performance of stopped-flow apparatus

The reaction of BSA and DTT proceeds at a suitable rate for testing the present small-angle equipment, SAXES. A single shot, as described here, of either 25 or 50 s time interval yields profiles of time-resolved measurements that can be analysed by Guinier plots. Accumulation of shots certainly makes experiments with time intervals of less than 1 s possible with similar accuracy, as well as improving scattering data with the present stopped-flow apparatus. However, the optics of SAXES projects a fairly large cross-section of incident X-rays on the specimen position, thus utiliz-

ing about 2/3 in the present specimen chamber. The chamber has a pair of 50 μm thick windows of quartz and reduces the X-rays to about 0.4 for $\lambda = 1.5$ Å. Since enlargement of the chamber cross-section and use of 20 μm thick windows may not disturb the present state of initial perturbation of a solution after mixing, i.e., cavitation and oscillation of X-ray path length, improvement of the stopped-flow chamber yields a 3-fold increase in X-rays. Together with the gain in intensity by changing the monochromators from silicon to germanium and improvement of the optics, the total intensity of the primary X-ray beam will be improved by about one order. Such improvement, as well as the use of greater protein concentration, makes the experiments with a time resolution of 100 ms or less possible with the SAXES in the Photon Factory in Tsukuba.

Acknowledgements

The authors are grateful to Professor Tadashi Matsushita of the Photon Factory Instrumentation Group, National Laboratory for High Energy Physics, for designing the optics and assistance in initial setting up of the SAXES. Thanks are also due to Dr. Hiroshi Nakatani of Kyoto University for his suggestion as to suitable conditions for the BSA-DTT for testing the performance of SAXES and the stopped-flow apparatus, and to Professor Masaru Sogami of Gifu University for discussion of the preliminary results. The authors would also like to thank the members of the Advisory Group of the molecular biology group headed by Professor Toshio Mitsui of Osaka University. Finally, they appreciate the continuous encouragement by Professors Kazutake Kohra and Taiji Sasaki of the Photon Factory, National Laboratory for High Energy Physics, Tsukuba.

References

1 R.S. Goody and K.C. Holmes, in: Use of synchrotron radiation in biology, ed. H.B. Stuhrmann (Academic Press, London, 1982) p. 203.
2 M.H.J. Koch, H.B. Stuhrmann, A. Tardieu and P. Vachette, in: Use of synchrotron radiation in biology, ed. H.B. Stuhrmann (Academic Press, London, 1982) p. 223.
3 G. Rosenbaum, K.C. Holmes and J. Witz, Nature 230, (1971) 434.
4 J. Barrington Leigh and G. Rosenbaum, Annu. Rev. Biophys. Bioeng. 5 (1976) 239.
5 J. Hendrix, M.H.J. Koch and J. Bordas, J. Appl. Crystallogr. 12 (1979) 467.
6 J. Bordas, M.H.J. Koch, P.M. Clout, E. Dorrington, C. Boullin and A. Gabriel, J. Phys, E: Sci. Instrum. 13 (1980) 938.
7 A. Gabriel, Rev. Sci. Instrum. 48 (1977) 1303.
8 T. Ueki, Y. Hiragi, Y. Izumi, H. Tagawa, M. Kataoka, Y. Muroga, T. Matsushita and Y. Amemiya, KEK Report (1985) in the press.
9 A. Guinier and G. Fournet, in: Small-angle scattering of X-rays (John Wiley and Sons, New York, 1955) p. 1.
10 O. Glatter and O. Kratky, in: Small angle X-ray scattering (Academic Press, London, 1982) p. 119.
11 J.R. Brown, 11th FEBS Meet. 50 (1977) 1.
12 T. Nagamura, K. Kurita and H. Kihara, 17th Meeting on Kinetics, Hiroshima (1982) A10.
13 J. Bordas, E.-M. Mandelkow and E. Mandelkow, J. Mol. Biol. 164 (1983) 89.
14 M.F. Moody, P. Vachette, A.M. Foote, A. Tardieu, M.H.J. Koch and J. Bordas, Proc. Natl. Acad. Sci. U.S.A. 77 (1980) 4040.
15 Y. Inoko, H. Kihara and M.H.J. Koch, Biophys. Chem. 17 (1983) 171.
16 B.K. Vainshtein, in: Diffraction of X-rays by chain molecules (Elsevier, Amsterdam, 1966) p. 173.
17 J.W. Anderegg, W.W. Beeman, S. Shulman and P. Kaesberg, J. Am. Chem. Soc. 77 (1955) 2927.
18 V. Luzzati, J. Witz and A. Nicolaieff, J. Mol. Biol. 3 (1961) 379.
19 J.F. Foster, in: The plasma proteins, vol. 1, ed. F. Putnum (Academic Press, New York, 1960) p. 179.
20 V. Bloomfield, Biochemistry, 5 (1966) 684.
21 W. Konigberg, Methods Enzymol. 25 (1972) 185.
22 D.L. Sondack and A. Light, J. Biol. Chem. 246 (1971) 1630.
23 A.S. Acharya and H. Taniuchi, J. Biol. Chem. 251 (1976) 6934.
24 H. Inouye, S. Era, S. Sakata, K. Kuwata and M. Sogami, Int. J. Peptide Protein Res. 24 (1984) 337.
25 M. Sogami, H.A. Peterson and J.F. Foster, Biochemistry 8 (1969) 49.
26 G.M. Edelman, W.E. Gall, M.J. Waxdal and W.H. Konigsberg, Biochemistry 7 (1968) 1950.